Developing a protocol for 3D-printable bioink from decellularised porcine tissue

Vendela Sandin

2023

Master thesis in Pharmaceutical technology

Department of Food technology

Faculty of Engineering, Lund University

LUND UNIVERSITY

Supervisor: Lars Nilsson

Assistant Supervisor: Morteza Aramesh

Examiner: Marie Wahlgren

Populärvetenskaplig sammanfattning

Grishud kan hjälpa vid cancerbehandling

Cancer är en av de vanligaste dödsorsakerna i Sverige idag och forskning om nya behandlingar utvecklas ständigt. En av dessa är immunterapi, där kroppens egna immunceller används för att attackera cancercellerna. I det här projektet har olika typer av grisvävnad använts för att skapa en gel som kan hjälpa immuncellerna nå tumörer.

Socialstyrelsen spår att mer än var tredje person kommer få en cancerdiagnos någon gång i livet. Tack vare forskningen har vi idag flera olika typer av behandling mot cancer, och cancerformer som tidigare ansågs obotliga har idag betydligt godare utsikter. Cancerforskningen utvecklas ständigt, och en relativt ny behandlingsmetod är så kallad immunterapi. Den går ut på att man odlar och tillför celler från kroppens egna immunförsvar som kan attackera cancercellerna. Det är framförallt en framgångsrik metod för att behandla olika typer av blodcancer. Ett problem uppstår dock när det gäller solida tumörer. Den koncentrerade samlingen cancerceller skapar en miljö som verkar hämmande på immuncellernas förmåga att attackera tumören. Men det kan finnas ett sätt att kringgå problemet: *Artificiellt vävnads-rekonstruktionsmaterial*. Det går ut på att, istället för att injicera immunceller direkt till tumörens närområde, låta dem växa i en typ av gel. Den gelen kan sedan opereras in vid tumören. Immuncellerna har då en gynnsam miljö varifrån de kan migrera till tumören. Men vilket material kan passa för att få cellerna att trivas?

Vävnaden i kroppen har två beståndsdelar. Den första är celler. Men det finns även någonting som kallas *extracellulärt matrix* (ECM). Det är den del av vävnaden som cellerna befinner sig i. Trots att ECM inte lever i någon biologisk mening kan den på kemisk nivå kommunicera med de celler som den omger. Den kommunikationen kan uppmuntra till bland annat celldelning och -migration.

Vid traditionell artificiell vävnadsrekonstruktion används material som är betydligt mindre komplext än ECM och saknar dessa kommunikationsvägar. I det här projektet har en artificiell vävnadsrekonstruktion som är gjort av ECM utvecklats. På det sättet kan komplexiteten av cellernas naturliga miljö behållas vilket förbättrar deras förmåga att bekämpa tumören. Gelen har dessutom egenskapen att den har en flytande form vid kallare temperaturer men stelnar när den värms upp till 37 ℃. Det innebär att den kan skrivas ut med en 3D-skrivare, vilket är ytterligare ett hjälpmedel att använda för att skräddarsy en vävnadsrekonstruktion som celler trivs i.

I det här projektet har tre olika grisvävnader använts för att tillverka en sådan gel: hud, aorta och vänster hjärtkammare. Genom att avlägsna cellerna från vävnaden erhålls ett ECM som kan lösas upp av enzymer i en sur miljö. Efter ett par dagar kan man få ut en vätska som blir till en gel vid kroppstemperatur. Den gelen kan bli grunden till nya framsteg i kampen mot cancer.

Abstract

T-cell administration via a scaffold is a promising tool for treatment of inoperable solid tumours. Traditional scaffold materials lack the complexity of the extracellular matrix (ECM) that cells normally grow in. An alternative is to instead use decellularised ECM (dECM) from biological tissue to create the scaffold. By making the scaffold via 3D-printing, its construction can also be a part of making it suitable for cells. This thesis aims to develop a protocol for decellularising a variety of tissues and using the dECM to make a printable biogel. The protocol was tested on three types of porcine tissue: aorta, left ventricle of heart, and skin. To be printable, it should behave as a liquid at 4 ℃ but display a storage modulus of at least 100 Pa when heated to 37 ℃. It should also have a shear thinning behaviour. All these objectives were attained. For characterisation of the dECM, assays to quantify the DNA content and glycosaminoglycane content were performed in order to determine decellularisation- and proteoglycans level respectively. However, no conclusive results were found in these assays.

Abstrakt

Administration av T-celler via en artificiell vävnadsrekonstruktion är en lovande metod för att behandla inoperabla tumörer. Traditionella vävnadsrekonstruktionsmaterial saknar den komplexitet som finns hos det extracellulära matrixet (ECM), där celler vanligtvis lever. Ett alternativ är då att använda decellulariserat ECM (dECM) som material när man skapar den artificiella vävnadsrekonstruktionen. Genom att använda en 3D-skrivare kan vävnadsrekonstruktionen ytterligare skräddarsys för cellers behov. Den här uppsatsen ämnar skapa ett protokoll för decellularisering som fungerar på flera olika typer av vävnad. dECM:et ska också användas till att skapa en biologisk gel som kan användas i en 3D-skrivare. Protokollet testades på tre olika typer av grisvävnad: aorta, vänster hjärtkammare och hud. För att kunna användas i en 3D-skrivare bör gelen vara flytande vid 4 ℃, men hårdna när den värms upp till 37 ℃. Viskositeten på gelen bör även minska när den utsätts för en kraft. Alla dessa mål uppfylls av gelen. Analys av DNA- och glygosaminoglykaninnehållet i dECM:et gjordes, dock utan brukbara resultat.

Contents

List of abbreviations

ECM	Extracellular matrix
dECM	Decellularised extracellular matrix
adECM	Aorta decellularised extracellular matrix
vdECM	Ventricle decellularised extracellular matrix
sdECM	Skin decellularised extracellular matrix
PBS	Phosphate-buffered saline
H&E	Hematoxylin and eosin
G’	Storage modulus
G’’	Loss modulus
GAG	Glycosaminoglycan
COL	Collagen
SDS	Sodium dodecyl sulphate
EDTA	Ethylenediaminetetraacetic acid

Introduction

Background

Treating cancer patients by administering T-cells - so called adoptive cell therapy - is a form of immunotherapy that in the last decade has been used to treat a growing number of cancers [1], [2]. While being a successful method for treating hematologic forms of cancer, some issues arrive when applying the method to solid tumours. For example, the microenvironment around the tumour acts inhibiting on the T-cell activity [3], [4]. One way to combat this is to administer the T-cells via a scaffold rather than injecting them into the environment close to the tumour. This technique has been shown to lower the risk of tumour relapse [5] compared to injection. However, as the migration and growth of cells are dependent on the environment in which they live [6], [7], the scaffold must provide a suitable environment for the cells for this to be a viable treatment. When making scaffolds, a common material to use is different gelatin or alginate mixtures. They do however fail to replicate the complexity of the extracellular matrix (ECM) that cells thrive in, as the ECM can interact with cells and thus affect cell behaviour [8], [9]. An alternative is to instead use a biogel made from decellularised ECM (dECM) when creating the scaffold. An environment much more like what cells are adapted to can thus be created [10]. An additional technique to further tailor the scaffold to the cell's liking is to, rather than seeding cells to a finished scaffold, add them to a pre-gel and then print a scaffold from the cell filled pre-gel using a 3D-printer, so-called bioprinting [11].

ECM composition and properties

What is left after decellularising most tissues is protein, mainly collagen. The peptides of collagen consist of a repeating pattern of amino acids: XaaYaaGly, meaning one third of the amino acids is a Glycine [12]. The Yaa position is commonly taken up by hydroxyproline, an amino acid almost uniquely found in collagen, where it accounts for around 13.5 % of the weight [13]. The peptide chains form triple helices that self-assemble into microfibrils. These fibrils can then cross-link into the collagen fibres that play a crucial part of tissue formation [12]. This cross-linking occurs due to the fact that the triple helices are unstable at body temperature and start to unfold at a micro level, which triggers the formation of collagen fibres [14]. Collagen, together with proteoglycan, forms the sturdy yet flexible network in which cells can thrive [15]. Proteoglycans are proteins conjugated to glycoseaminoglycan (GAG) chains. These chains affect the possible chemical interactions [16] and can be used for identification [17]. GAGs can also interact with proteins and affect, among other things, cell growth and migration [18].

Gel composition and properties

A successful pre-gel should be liquid in cool temperatures in order to be printable, and form the gel when reaching 37 ℃. The physical properties of a substance can be measured with a

rheometer that determines the storage modulus and loss modulus. These describe the solid- and liquid-like properties of the substance, respectively. A high storage modulus (G') of the gel is vital for it to keep the printed shape [19]. At 37 ℃, the storage modulus should be higher than the loss modulus (G''). It should also reach a value of at least 100 Pa in order to match the stiffness of soft tissues in the body [20], [21]. To achieve printability, the pre-gel should however display a lower G' and a relatively high G''. It should also display shear-thinning properties; a lower viscosity when experiencing force [19].

Decellularising tissue

The first step when creating a bioink from tissue is to remove the cells so that only the extracellular matrix (ECM) remains. This can be achieved using physical, chemical and enzymatic means [22], [23]. The most common strategy to obtain decellularised ECM (dECM) is through chemical means. The bi-lipid cell membrane is disrupted using using ionic and non-ionic detergents that lyse the cells, like sodium dodecyl sulphate (SDS) and Triton X-100, respectably [22]-[25]. Some research indicate that even just phosphate-buffered saline (PBS) can help decellularise the tissue [23]. The ECM can be considered decellularised when the DNA content is lower than 50 ng/mg dry weight and when cell staining such as H&E (Hematoxylin and Eosin) does not yield visible nuclear material. A common finishing step is to immerse the decellularised tissue in peracetic acid. The acidic environment can help decellularisation process, but it is its oxidising properties that are used to disinfect the dECM [23].

Aim

The aim of this project is to, with an existing protocol [8] as a basis, develop a protocol for the preparation of bioink from the ECM that can be used on a variety of tissues. The protocol will be tested on the aorta and left ventricle of porcine heart, as well as on porcine skin. The amount of decellularisation will be measured via DNA analysis. The dECM will also be characterised by the remaining amount of GAG, collagen, and the shear thinning properties of the pre-gel. The gelation of the pre-gel will be evaluated by its rheology.

Methods and materials

Method development

Decellularisation of tissue

When homogenising the tissue, three different methods were tested: cutting using a scalpel, mixing with a household blender, and using a blade coffee grinder. The goal was to achieve as small pieces as possible.

During development of the protocol, results were evaluated by visual results, mainly if the tissue turned white throughout during decellularisation. The main variable that was changed was the liquid-to-tissue ratio. The aim was to have it as small as possible, as that allows for a more economic procedure. For the ventricle tissue, one 15-minute rinse was added before the treatment to remove blood.

Preparation of pregel

When developing the protocol, the quality of the pregel was measured based on gelation via a rheometer. If G' needed to be increased, a higher concentration of dECM-to-acetic acid was used. The pepsin-to-dECM ratio was constant and based on literature [8] with the exception of one trial with 1/10 of the determined ratio was tested in order to evaluate the possibility of using less pepsin.

Protocol

Decellularisation of tissue

Compound	**Quality**	**Purchased from**
PBS, 10X Solution	Molecular Biology Grade	Thermo Scientific Chemicals
Sodium Dodecyl Sulfate (SDS)	Standard grade	Thermo Scientific Chemicals
Triton™ X-100	Laboratory grade	Merck
Acetic acid	ACS grade	Merck
Hydrogen peroxide 30%	M200	Sigma-Aldrich
Purified water	Type I water	Milli-Q QPAK®

To prepare the tissue, grind it into a paste. If the tissue is too tough for this, e.g. aorta, instead cut it into small pieces. Weigh the tissue; the ratio of tissue-to-washing liquid should be about 10 ml liquid per gram tissue (see Note 1). Remove excess material, e.g. grease, that has separated from the tissue between each wash. See appendix for notes.

1. If the starting tissue contains a lot of washable substances, e.g. blood in muscle tissue, wash in a beaker of PBS for 15 minutes (see Note 2).
2. Dissolve 1 wt% SDS in PBS. Mix until completely dissolved.
3. Transfer the tissue to the SDS solution. Wash while stirring for 48 hours.

4. Dissolve 1 wt% Triton X-100 in ultrapure water (see Note 3).
5. Transfer tissue to the Triton X-100 solution (see Note 2). Wash while stirring for 30-45 minutes.
6. Transfer the tissue to a beaker with PBS (see Note 2). Wash while stirring for at least 3 days.
7. Prepare a mixture of 1 vol% acetic acid and 3 vol% hydroperoxide.
8. Transfer the tissue to the prepared mixture (see Note 2) and wash while stirring for 2 hours.
9. Transfer the tissue into a PBS solution (see Note 2). Wash while stirring for 15 minutes. Repeat once.
10. Transfer the tissue to ultrapure water (see Note 2). Wash while stirring for 15 minutes. Repeat once.
11. Remove the tissue from the water.
12. Freeze-dry until completely dry.
13. Grind the dECM into a powder.
14. Store at -20 ℃.

Preparation of pregel:

Compound	**Quality**	**Purchased from**
Acetic acid	ACS grade	Merck
Pepsin	Proteomics Grade	Sigma-Aldrich
Milli-Q	Type I water	Milli-Q QPAK®
NaOH	Reagent grade	Sigma-aldrich

1. Measure up the amount of dECM that will be used.
2. Prepare 0.5 M acetic acid and mix with 1 mg pepsin per mg dECM (see Note 4).
3. Transfer the dECM to the pepsin solution.
4. Incubate at 4 ℃ for 48-72 hours (see Note 5) while revolving (see Note 6).
5. For dECM without greasy residue:
    a. If not all dECM is fully dissolved, centrifuge at 1000 g for 5 minutes and transfer the supernatant into a clean tube.
    b. Adjust pH to 7.2 ± 2 using 10 M NaOH (see Note 7). The temperature of the pre-gel should not exceed 10 ℃ (see Note 8).
6. For dECM with greasy residue:
    a. Centrifuge at 1000 g for 5 minutes
    b. Remove the separated top layer

c. Transfer the liquid to a clean container (see Note 9)
d. Adjust to pH 7.2 ± 2 with 10 M NaOH (see Note 7). The temperature of the pre-gel should not exceed 10 ℃ (see Note 8).
e. Centrifuge at 1000 g for 4 minutes
f. Transfer the liquid to a clean container (see Note 9)

7. Use immediately or store at 4 ℃ (see Note 10).

Characterisation of ink

GAG and DNA preparation

To prepare the tissue for GAG and DNA analysis, the freeze dried dECM was added to a papain solution. To prepare that solution, 125 µg papain/mL was added to a solution containing 0.1 M sodium dihydrogen phosphate monohydrate, 5 mM Na_2-EDTA (Ethylenediaminetetraacetic acid), and 5 mM cysteine-HCL. The solution was prepared by first dissolving EDTA at pH 8. The cysteine was dissolved in a separate container with MilliQ-water and added to the EDTA solution. After that, the sodium phosphate and milliQ-water to the desired volume was added. The solution was then pH-adjusted using 10 M NaOH until a pH of 6.5 was reached. For the DNA analysis, 10-15 mg of each tissue was digested in 0.3 ml of the papain solution. For the GAG analysis, similar amounts were used, but a concentration of 50-55 mg/ml dECM was obtained. The tissue was incubated in the papain solution for 16 h at 60 °C with agitation. Samples that had not completely dissolved after the 16 hours were left for an additional two hours. The samples were then centrifuged for 3 minutes at 10 000 g, and the supernatant was extracted and used in analysis. Freeze-dried tissue that had only gone through the first SDS wash underwent the same preparation and was used as a reference.

DNA analysis

Compound	**Quality**	**Purchased from**
Hoechst 33258 solution	MQ 100	Sigma.-Aldrich
Deoxyribonucleic acid sodium salt from calf thymus	MQ 300	Sigma-Aldrich
PBS, 10X Solution	Molecular Biology Grade	Thermo Scientific Chemicals
Purified water	Type I water	Milli-Q QPAK®

DNA content was measured in triplicates using a Hoechst 33258 assay on a 96-well plate. 250 uL of the prepared supernatant was added to each well. 3.8 uLof Hoechst 33258 solution, making a well concentration of 15 ug/mL Hoechst 33258. The plate was incubated for 15 minutes before being read using an excitation wavelength of 360 nm and an emission wavelength of 454 nm.

A standard curve was made at a later time using 2.5 mg calf thymus DNA dissolved in 20 mL of the papain solution. The dissolved DNA was diluted using a dilution series, making a standard curve spanning from 125 to 6.05 ug/mL. 250 uL of each dilution was added to a 96-well plate. 15 uL of Hoecht 33258 was added to each well. The plate was incubated for 15 minutes before being read using an excitation wavelength of 360 nm and an emission wavelength of 454 nm.

GAG analysis

Compound	Quality	Purchased from
Chondroitin sulphate sodium	MQ 300	Sigma-Aldrich
1,9-Dimethyl-Methylene Blue zinc chloride double salt	MQ 200	Sigma-Aldrich
Glycine	MQ 200	Sigma-Aldrich
PBS, 10X Solution	Molecular Biology Grade	Thermo Scientific Chemicals
NaCl	Unknown	Unknown
Acetic acid	ACS grade	Merck
Purified water	Type I water	Milli-Q QPAK®

GAG content was measured using 1,9-dimethylmethylene blue (DMMB). DMMB reagent was prepared by dissolving 8 mg DMMB, 1.52 g glycine, 0.8 g NaCl, and 0.54 ml glacial acetic acid in Milli-Q water and completing the volume to 0.5 L. The reagent was then filtered through a 0.45 µm filter and stored away from light. For the standard curve, 500 mg chondroitin sulphate sodium was dissolved in 5 mL MilliQ-water, creating a 0.1 mg/mL standard solution. This was further diluted to a 500 µg/ml solution. The standard solution was then transferred to a 96-well micro plated according to table 1. 20 µL of each sample was transferred onto the 96-well plate in triplicates. After that, 200 µL DMMB solution was added to all plates and the plate was immediately read at 525 nm.

Table 1: Variables when making the standard curve used for the GAG analysis

Concentration [µg/ml]	Standard solution volume [µL]	Papain solution [µL]
0	0	20
1.25	2.5	17.5
2.5	5	15
5	10	10
7.5	15	5
10	20	0

Shear thinning

The shear thinning properties of the pre-gel was tested using a Discovery HR 10 rheometer with a 20.0 mm diameter stainless steel plate. The following parameters were used:

- Volume: 500 µL
- Gap: 500 µm
- Temperature: 4 ℃
- Shear rate: 0.1 /s to 100.0 /s
- Equilibration time: 6.0 s

Gelation

Electron microscopy

Pre-gels from the three different tissues were placed in 37 ℃ for one hour to gel. They were then freeze dried and analysed using a scanning electron microscope (SEM).

Rheology

The rheology analysis was performed immediately after the shear thinning analysis using the same equipment. A 5 minute wait time at 4 ℃ between analyses was introduced to let the gel stabilise. The frequency-dependent storage (G') and loss (G'') was measured using the following parameters:

- Temperature 37 ℃
- Soak time: 0 s.
- Soak time after ramp: 0 s.

- Strain: 0.6 %
- Frequency: 1.0 Hz
- Angular frequency: 6.28319 Hz.
- Torque: 0.1 μNm

The analysis was terminated when it had reached its plateau or when the gel had dried. Duplicates were made on each sample. All three gel types were tested at a pH of 7.2 ± 0.2 at the day of pH-adjustment. Gel from skin dECM (sdECM) was also analysed one day after pH-adjustment at 4 different pH-values: 7.446, 9.235, 10.150, and 12.087. All analyses were done in duplicates.

Results

Method development

Decellularisation of tissue

The chosen liquid-to-tissue ratio that did not affect signs of decellularisation was 10 mL liquid/g tissue.

Preparation of pregel

A ratio of 30 mg sdECM and 7.5 a/vdECM per ml acetic acid was established. The lower amount of pepsin did not adequately dissolve the dECM.

Characterisation of ink

DNA analysis

The standard curve that was created made an S-shaped curve (see figure 1). The majority of the measured values were not within the linear range and could thus not be quantified. A highly approximative placement of the samples and reference results has been placed on the curve. These measurements are only relevant for the concentration of DNA in the supernatant of the dissolved samples, whose tissue-to-solvent varied measured. The results can thus not be directly translated to tissue- or dECM DNA content. All samples did however display a significant decrease in fluorescence after decellularisation (figure 2). The decrease in fluorescence intensity of the aorta dECM (adECM) was 94 %, that of ventricle dECM (vdECM) 96 %, and the sdECM displayed a 83 % decrease. However, these values can only be used to infer a pattern and can not be considered as correct values, as the concentration-to-fluorescence intensity correlation is not linear within the range measured. One thing that can still be noted is that while the sdECM had the lowest percentual decrease

of the three tissues, the total value was the lowest, as it had a much lower starting concentration than the others (figure 1).

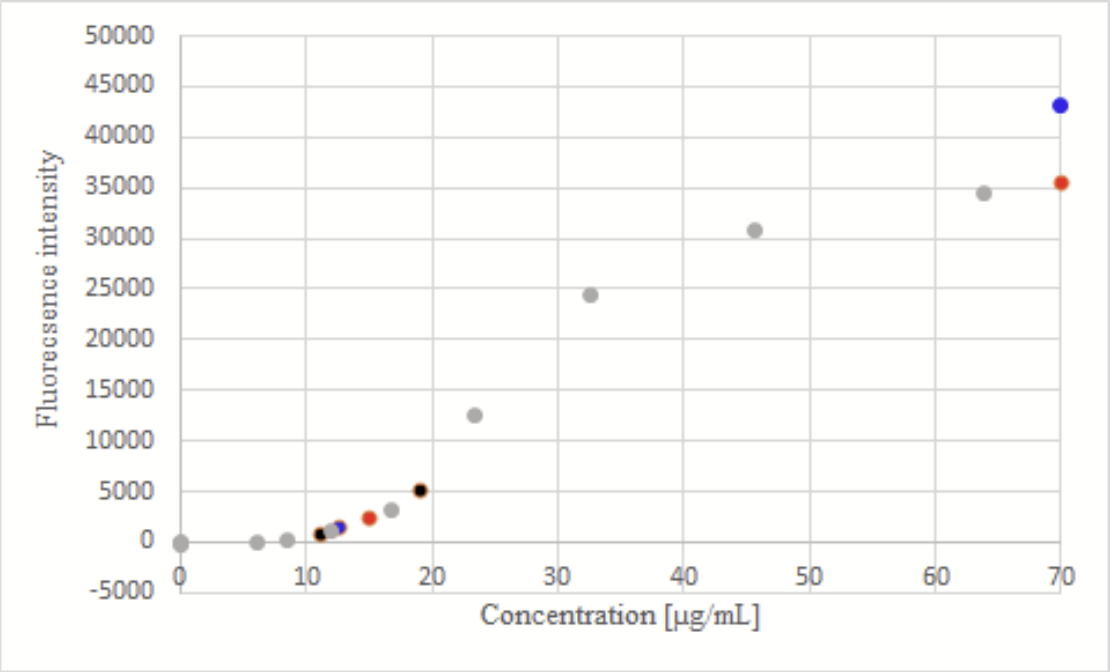

Figure 1: The standard curve for DNA quantification with the samples added, where the x–axis position is determined by visual approximation. The grey dots represent the standard curve. The two samples originating from aorta are blue, the ones from ventricle are red, and the ones from skin are black. All tissues displayed a decreased intensity after decellularisation.

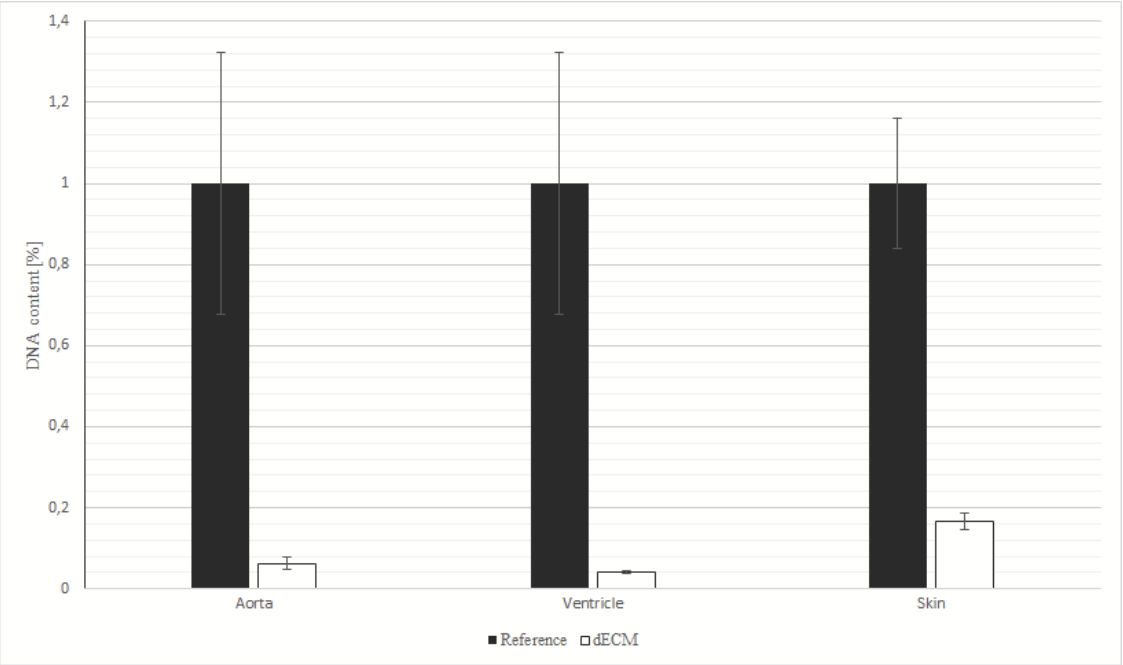

Figure 2: The difference in fluorescence intensity before and after decellularisation for aorta, ventricle and skin tissue. The values of each tissue has been adjusted according to the tissue concentration in the dissolved sample.

GAG analysis

The values of all samples were below the range of the standard curve. The absolute values could thus differ significantly from the true ones. It does however show that while the concentration of GAGs decreased after decellularisation, the concentration in the two heart tissues increased (figure 3).

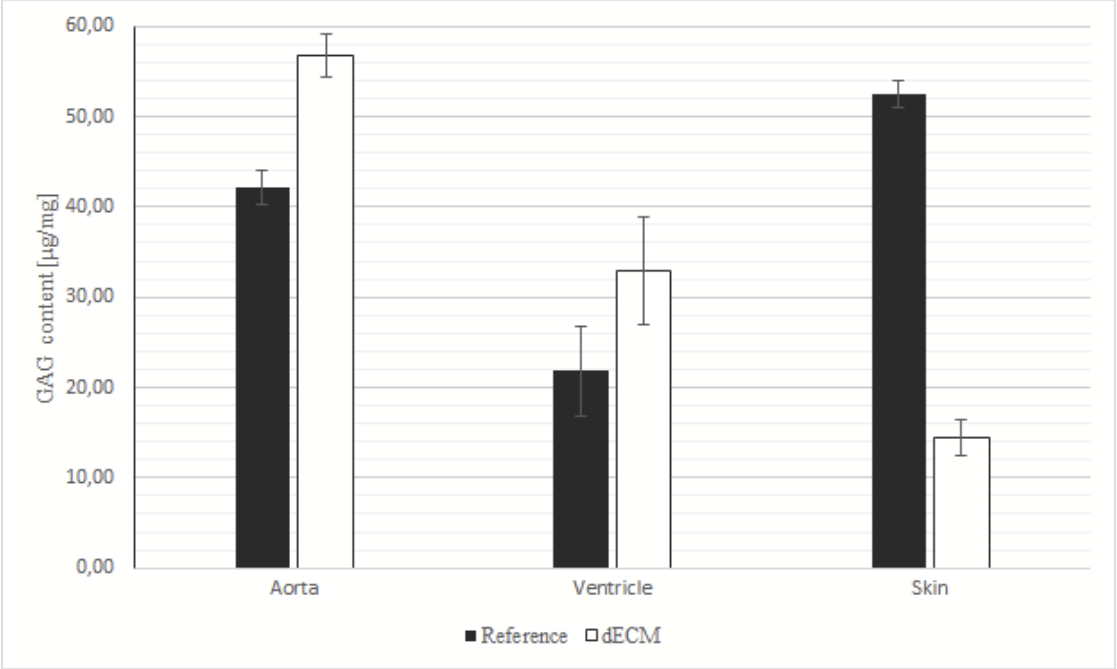

Figure 3: Difference in GAG content for dECM of aorta, ventricle, and skin compared to non-decellularised tissue. All values have been adjusted to represent the concentration in dry tissue.

Shear thinning

According to figure 4, the heart tissues displayed a visible shear thinning in the range 0.01-100 s^{-1}. The adECM went from 4.54 Pa×s to 0.093, and the vdECM from 0.93 to 0.057 Pa×s. The sdECM showed no clear shear thinning pattern.

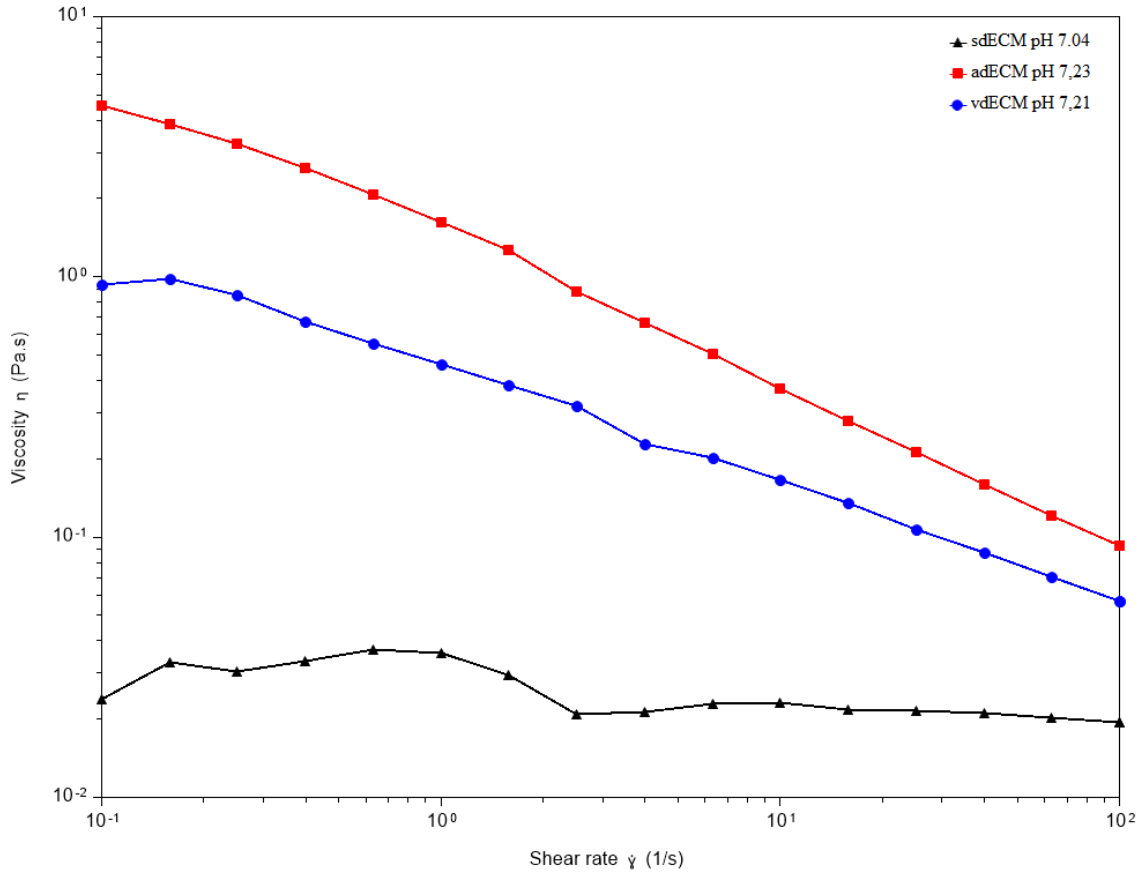

Figure 4: Shear thinning properties of the different dECMs.

Gelation

Electron microscopy

See figure 5 for SEM images.

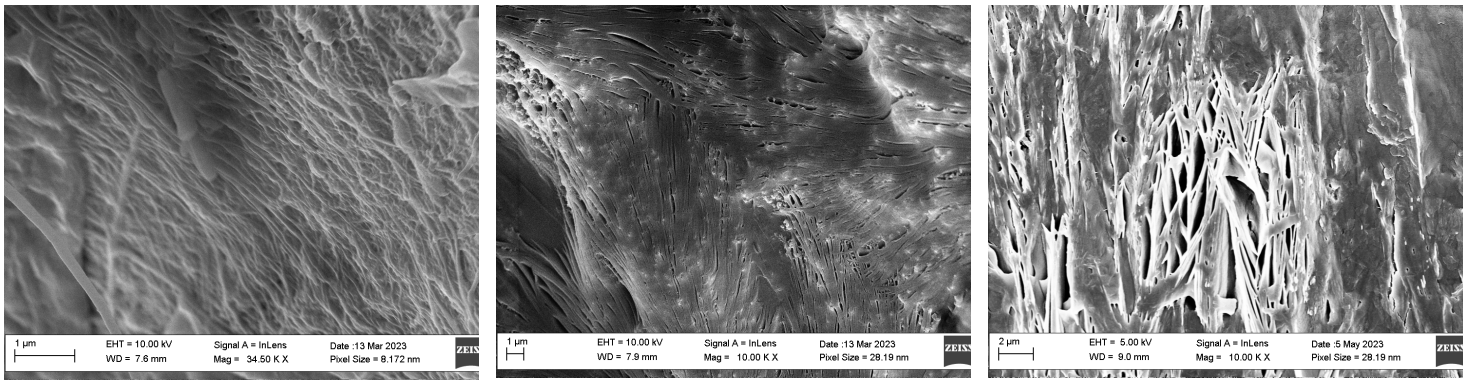

Aorta Ventricle Skin

Figure 5: Gel made from the dECM of aorta, ventricle and skin viewed from a SEM.

Rheology

Tissue dependence

The results of the rheological analysis can be seen in figure 6. All pre-gels visibly gelled when heated up to 37 ℃ (figure 7). For all samples, the storage modulus exceeded their loss modulus very early in the gelation process, but they both continue to increase during the gelation. The adECM gel reached G' of 3085 Pa when it plateaued at 31 minutes. The vdECM gel similarly reached 1158 Pa in 32 minutes. The sdECM gel peaked at 186 Pa at 35 minutes, after which it flattened out to 94 Pa.

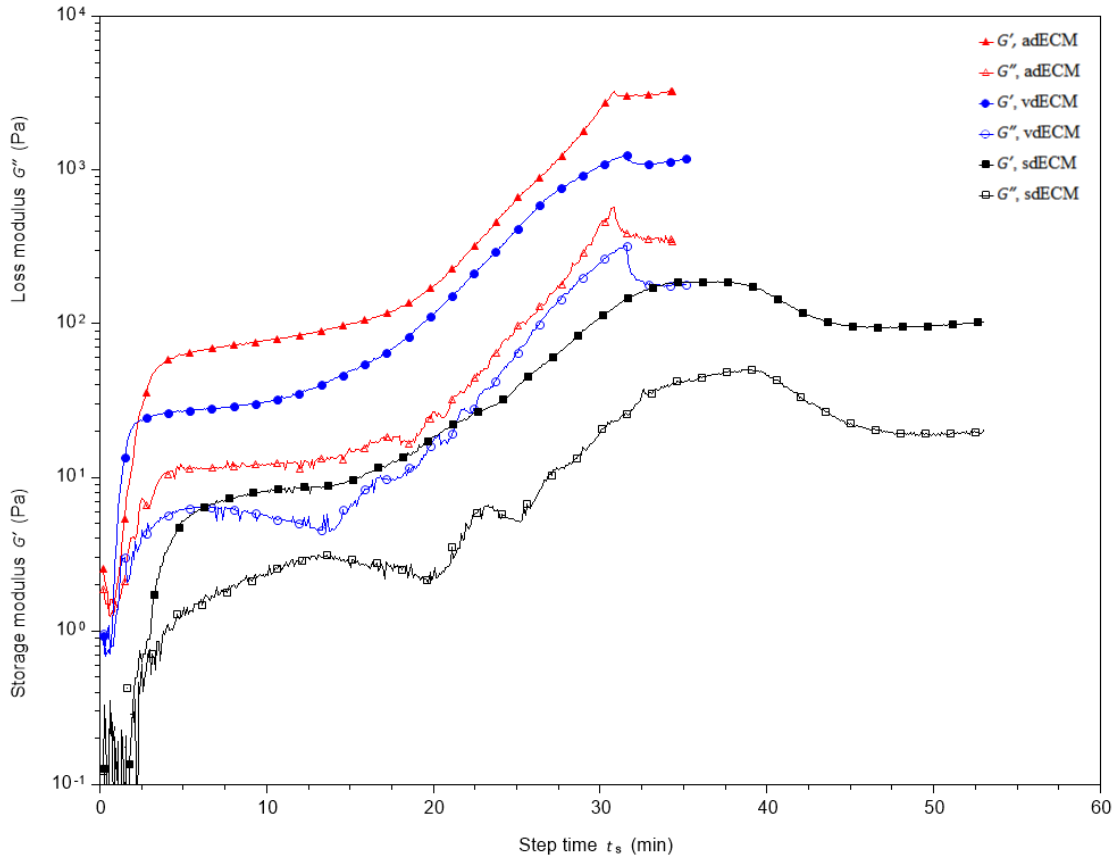

Figure 6: The rheological analysis of the gelation of gel made from adECM, vdECM, and sdECM. At $t_s = 0$, the temperature was 4 ℃ which was increased to 37 ℃ within the first few minutes of the analysis.

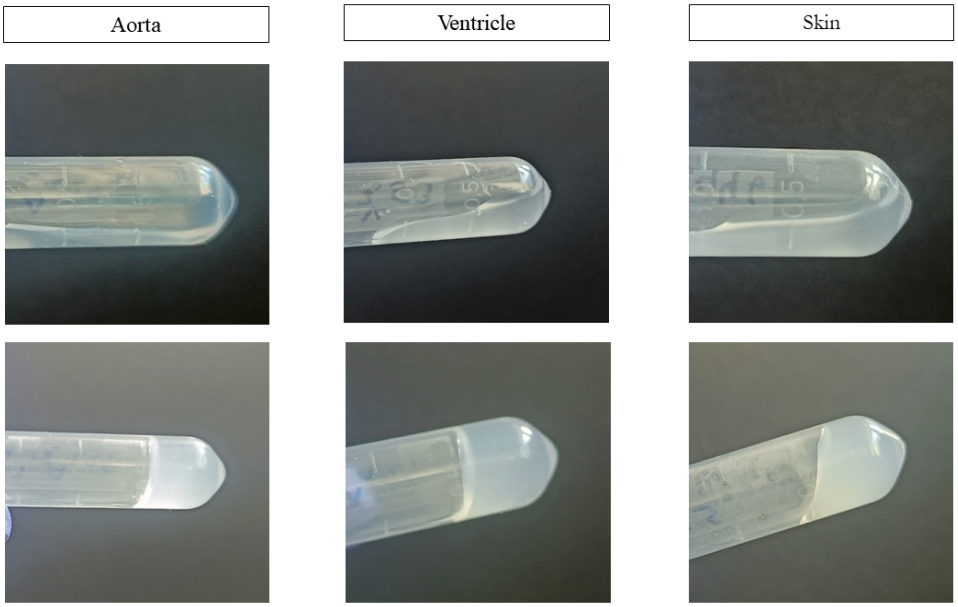

Figure 7: Visual changes in consistency between the pre-gels (top) and gels (bottom).

pH dependence

Table 2 shows the maximum G' each gel reached and the time it took. The exception being the pH 10.15 gel that did not display an apex. Instead, the last point before the sudden increase was chosen, as the change in behaviour most likely is due to drying rather than gelation. Figure 8 shows the changes in G' when the pre-gel is heated to 37 ℃.

Table 2: Gelation level measured by G' and the gelation time for pre-gel made from sdECM at four different pH levels.

pH of gel	G' maxima [Pa]	Time [min]
7.45	440	34
9.24	110	30
10.15	77	39
12.09	420	35

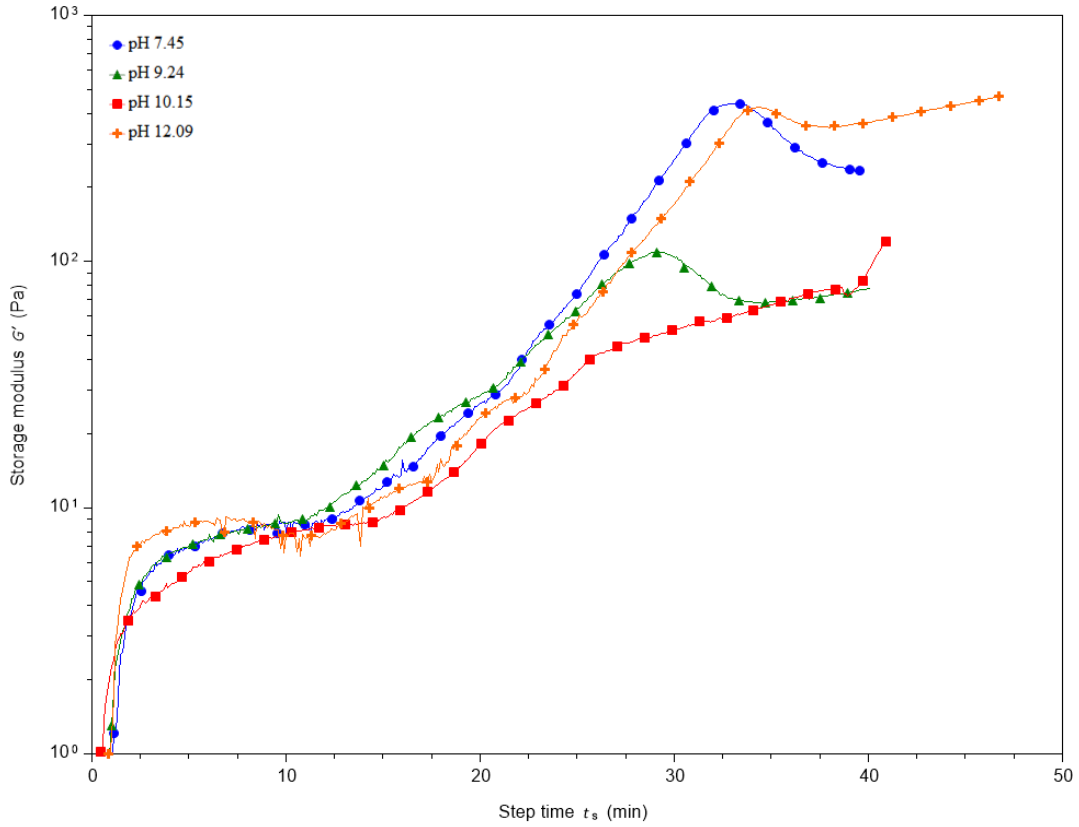

Figure 8: The gelation for pre-gel made from sdECM at four different pH levels.

Discussion

Method development

Decellularisation of tissue

The materials used in this protocol were mostly the same as those used in the established one [8]. Adjustments were done to optimise the volumes and proportions of the different steps, and to develop a method to rid the pre-gel of impurities. One change in substance was to substitute peracetic acid to a acetic acid-hydrogen peroxide mixture. It was done to simplify the procedure as peracetic acid is generally a more unavailable substance than the others. It should be noted that the change to an acetic acid-hydrogen peroxide mixture does not have explicit support in literature, so it is possible that it is not adequately disinfected. If further research concludes that it is not a viable habitat for cells, this could be the missing step.

Visually, the vdECM stood out as it had a darker shade than the other two dECMs. While both adECM and sdECM became white after washing, the vdECM had a grey discolouration that could not be removed. A reason for this could be that the ventricle contains many other proteins that were not removed during the washing process. They could

also cause the lower G' when compared to the gel of the same concentration made from adECM.

Preparation of pregel

The sdECM contained some fat that did not get dissolved in the acetic acid and pepsin solution. This resulted in both small and large fat particles dispersed throughout the gel. The majority of these could be removed after the dissolution phase using centrifugation. However, there were still small particles creating a white opaque colour of the pre-gel. Curiously, this could be resolved by a second centrifugation when the pre-gel had a pH of between 7 and 9. Higher and lower pH:s seemed to somehow affect the particle behaviour as all residue could not get separated in those cases.

The heart dECMs also caused some problems when dissolving. Here, the issue was not so much residues, as it was partly undissolved pieces even after extending the incubation time. This yields not only an uncertain final concentration, but they were also much more difficult to separate from the functioning pregel. Centrifugation helped some, but in order to avoid the un- or half dissolved pieces, a lot of pre-gel had to be discarded. To combat this, the dECM could be more finely grinded, into a powder, so that the larger surface area helps dissolve the pieces more efficiently. However, if the reason is that the acetic acid was saturated with protein, the remedy would be to use a lower initial concentration. This would mean that the G' reached in this experiment most likely is close to the maximum possible when using this protocol on the aorta and ventricle of the porcine heart. Further experiments using a lower concentration can resolve this question. With the G' reached here, it is usable on soft tissue as was the goal.

Characterisation of ink

GAG analysis

While the GAG content was predictably lower in the sdECM after decellularisation, it was surprisingly higher in both heart tissues. This could be attributed to the fact that a higher amount of other materials were washed away than GAGs. That would mean that even though the absolute amount of GAG is lower after decellularisation, it takes up a higher relative amount of the mass. Interestingly, the sdECM has a high amount of GAG before decellularisation, even though it is suspected to have a lower proportion of proteins than the heart tissues due to its fat content. The fact that GAGs could be discovered using this assay is a good sign, as the decellularisation did not wash them all away.

COL analysis

The COL analysis did not yield any results. However, while not a part of this thesis, mass spectrometry and SDS-PAGE were performed on the different gels and they both support presence of collagen in the gel (see appendix A2-A3). The gelling process itself also implies that the gel contains collagen.

DNA analysis

A quantitative result could not be obtained from the DNA analysis. Since the analysis was done in triplicates that clearly displayed a pattern, it can still be inferred that the tissue is greatly decellularised though it is unknown as to what level. Based on the level of fluorescence intensity however, there is a possibility that the dECM's are not completely decellularised. An initial adjustment to the protocol could be to replace the washing solution daily. If there are cells still in the dECM, another decellularising step could be added. To create a more rounded decellularisation, this could be for example physical or enzymatic.

Shear thinning

The heart tissues displayed the expected and desired shear thinning. The sdECM, however, did not. The duplicates did however indicate that the shape is not random, and the viscosity has a maxima somewhere between 0.6 and 0.8 s^{-1}. In the measured pre-gel, the lack of shear thinning is not necessarily an issue, as it is soft enough to be printable as it is. It could however be further analysed how more concentrated sdECMs respond to shear stress.

Gelation

Electron microscopy

The gel from adECM displayed fibrous structures, which could be collagen fibres. Gel from vdECM had a layered structure, similar to sheets stacked on top of each other. sdECM Was also layered, but the sheets are connected like a network.

It should be noted that these images were created on an early iteration of the protocol, making them, in particular the adECM, promising for the future.

However, the image from the adECM gel displays what could be bacteria. Even though it is not likely that a relevant amount of bacteria has survived the protocol, it serves as a reminder that since the starting material is biological tissue, measures must be taken to minimise the amount of contaminants.

Rheology

The gelation was successful for all three tissues as they all reached a G' that is above 100 Pa and higher than the loss modulus. An upper limit on G' is not necessarily a requirement, as the pre-gel can be diluted with e.g PBS to combat a gel that is too hard.

When comparing the shapes of the curves, it is apparent that the sdECM follows a different pattern than the others. This could be due to different behaviour at different G' as it has a much lower value than the others, or it could have something to do with the drying process of the gels. If evaporation during analysis could be avoided or minimised, it is possible that the curves would look different. Within this thesis the heart based gels seem to be the odd ones out as most experiments used sdECM based gel but when looking at other literature storage modulus curves without the apex can be seen [8], [26]. Since most

measurements of the sdECM gel follows the same pattern, it could be other substances from the skin that affect the gelling properties.

The significantly lower G' of the sdECM can also be seen through the lens of concentration of dECM-to-acetic acid when making the pre-gel. The concentration of the sdECM was 30 mg/ml, while the concentration of the adECM and vdECM was 7.5 mg/ml. Presumably, a higher concentration of tissue should mean a higher concentration of collagen, and thus, a harder gel. This can be explained by the fact that while the heart tissues don't appear to contain much else than protein, the sdECM did clearly contain fat. The fat was discarded via centrifugation of the pre-gel but this means that the actual concentration of functioning sdECM is lower than the initial one. Due to the undissolved parts previously mentioned, it is also not clear what the concentration of the heart based gels are.

It was noticed during analysis that the gelation of the pre-gel was somewhat time sensitive. In order minimise the time dependence of the gelation process when comparing pH variations, the pH-adjustments were performed one day prior to the analysis as each analysis lasted about an hour and only one sample could be tested at a time. The samples were stored at 4 ℃ overnight and analysed the next day. Time did however also affect the pH of the pre-gel, especially when the initial pH was high. It is therefore not likely that the pH values depicted here were still accurate. The following discussion does however assume that, while the absolute values might not be correct, the relative pH values within the sample group stay consistent over time.

When comparing the pH-dependence of the gels two things stand out. The first is that the gel with a pH of 10.15 does not follow the same gelation pattern as the others. The analysis of that sample was done in triplicates, and the same shape could be seen in all three trials. One flaw in that analysis was that the sample with pH 10.15 had been adjusted one day prior to the others, but then to a pH of 11.72. One theory could be that the time aspect affects the shape of the curve. However, even when measured right after being adjusted to pH 11.72, the shape that is very similar to those in the protocol [8] this thesis is based on could be seen (see appendix A1). The other notable thing is that while it in the beginning seems like the G' of the gel decreases with a higher pH, that pattern is abruptly broken with the pH 12.09 gel closely following the shape of the 7.45 gel. This interesting pattern could be subject to further investigation, but since the gel is thought to be used as a reservoir for cells and inserted into biological tissue, a more in depth analysis of a physiological pH is likely a more worthwhile endeavour.

Conclusion

The protocol developed provides a good base for future research on tissue-based printable biogels. The protocol would need some improvement to optimise yield when used on heart tissue. Skin tissue is however a good fit for this protocol, and the gel created from this can be adjusted via sdECM concentration, pH, and incubation after pH-adjustment to achieve desired properties. The results of DNA and GAG quantification are promising, but other assays are needed to determine the true amounts. The next steps in developing this gel further is to test its printability with a 3D-printer and looking at cell compatibility.

References

[1] J. D. Chan, J. Lai, C. Y. Slaney, A. Kallies, P. A. Beavis, and P. K. Darcy, “Cellular networks controlling t-cell persistence in adoptive cell therapy,” Nature Reviews Immunology, vol. 21, no. 12, pp. 769–784, 2021.

[2] J. C. Yang and S. A. Rosenberg, “Adoptive t-cell therapy for cancer,” Advances in immunology, vol. 130, pp. 279–294, 2016.

[3] K. Kirtane, H. Elmariah, C. H. Chung, and D. Abate-Daga, “Adoptive cellular therapy in solid tumor malignancies: review of the literature and challenges ahead,” Journal for immunotherapy of cancer, vol. 9, no. 7,2021.

[4] A. M. A. Rømer, M.-L. Thorseth, and D. H. Madsen, “Immune modulatory properties of collagen in cancer,” Frontiers in Immunology, vol. 12, 2021. [Online]. Available: https://doi.org/10.3389/fimmu.2021.791453

[5] S. B. Stephan, A. M. Taber, I. Jileaeva, E. P. Pegues, C. L. Sentman, and M. T. Stephan, “Biopolymer implants enhance the efficacy of adoptive t-cell therapy,” Nature Biotechnology, vol. 33, 2014. [Online]. Available: https://doi.org/10.1038/nbt.3104

[6] P. Lu, K. Takai, V. M. Weaver, and Z. Werb, “Extracellular matrix degradation and remodeling in development and disease,” Cold Spring Harbor Perspectives in Biology, vol. 3, no. 12, 2011. [Online]. Available: https://doi.org/10.1101/cshperspect.a005058

[7] J. Lopez, J. Mouw, and V. Weaver, “Biomechanical regulation of cell orientation and fate,” Oncogene, vol. 27, no. 55, 2008. [Online]. Available: https://doi.org/10.1038/onc.2008.348

[8] F. Pati, J. Jang, D.-H. Ha, S. W. Kim, J.-W. Rhie, J.-H. Shim, D.-H. Kim, and D.-W. Cho, “Printing three-dimensional tissue analogues with decellularized extracellular matrix biolink,” Nature Communications, vol. 5, no. 3935, 2014. [Online]. Available: https://doi.org/10.1038/ncomms4935

[9] T. Walimbe and A. Panitch, “Proteoglycans in biomedicine: resurgence of an underexploited class of ecm molecules,” Frontiers in Pharmacology, vol. 10, p. 1661, 2020.

[10] R. A. Pouliot, B. M. Young, P. A. Link, H. E. Park, A. R. Kahn, K. Shankar, M. B. Schneck, D. J. Weiss, and R. L. Heisse, “Porcine lung-derived extracellular matrix hydrogel properties are dependent on pepsin digestion time,” Tissue Engineering Part C: Methods, vol. 26, no. 6, 2020. [Online]. Available: https://doi.org/10.1089/ten.tec.2020.0042

[11] J. Kundu, J.-H. Shim, J. Jang, S.-W. Kim, and D.-W. Cho, “An additive manufacturing-based pcl–alginate–chondrocyte bioprinted scaffold for cartilage tissue engineering,” Journal of tissue engineering and regenerative medicine, vol. 9, no. 11, pp. 1286–1297, 2015.

[12] M. D. Shoulders and R. T. Raines, “Collagen structure and stability,” Annual review of biochemistry, vol. 78, pp. 929–958, 2009.

[13] R. E. Neuman, M. A. Logan et al., “The determination of hydroxyproline,” J Biol Chem, vol. 184, no. 1, pp. 299–306, 1950.

[14] E. Leikina, M. Mertts, N. Kuznetsova, and S. Leikin, “Type i collagen is thermally unstable at body temperature,” Proceedings of the National Academy of Sciences, vol. 99, no. 3, pp. 1314–1318, 2002.

[15] F. Dehghani and A. Fathi, “Challenges for cartilage regeneration,” in Biomaterials for Implants and Scaffolds, Q. Li and Y.-W. Mai, Eds. Berlin, Germany: Springer, 2017, p. 390. [Online]. Available: https://doi.org/10.1007/978-3-662-53574-5

[16] R. V. Iozzo and L. Schaefer, “Proteoglycan form and function: A comprehensive nomenclature of proteoglycans.” Matrix Biology, vol. 42, pp. 11 – 55, 2015. [Online]. Available: https://ludwig.lub.lu.se/login?url=https://search.ebscohost.com/login.aspx?direct=true&AuthType=ip,uid&db=edselp&AN=S0945053X15000402&site=eds-live&scope=site

[17] D. Xu, J.H Prestegard, R.J. Linhardt, et al. Proteins That Bind Sulfated Glycosaminoglycans. In: Varki A, Cummings RD, Esko JD, et al., editors. Essentials of Glycobiology [Internet]. 4th edition. Cold Spring Harbor (NY): Cold Spring Harbor Laboratory Press; 2022. Chapter 38. Available: https://www.ncbi.nlm.nih.gov/books/NBK579914/ doi: 10.1101/glycobiology.4e.38

[18] G. Kimbell and M. A. Azad, “Chapter fifteen - 3d printing: Bioinspired materials for drug delivery.” Bioinspired and Biomimetic Materials for Drug Delivery, pp. 295 – 318, 2021. [Online]. Available: https://ludwig.lub.lu.se/login?url=https://search.ebscohost.com/login.aspx?direct=true&AuthType=ip,uid&db=edselp&AN=B9780128213520000113&site=eds-live&scope=site

[19] G. Fallenstein, V. D. Hulce, and J. W. Melvin, “Dynamic mechanical properties of human brain tissue,” Journal of biomechanics, vol. 2, no. 3, pp. 217–226, 1969.

[20] J. Liu, H. Zheng, P. Poh, H.-G. Machens, and A. Schilling, “Hydrogels for engineering of perfusable vascular networks,” International Journal of Molecular Sciences, vol. 16, pp. 15 997–16 016, 2015.

[21] M. S. Islam, A. Aryasomayajula, and P. R. Selvaganapathy, “A review on macroscale and microscale cell lysis methods,” Micromachines, vol. 8, no. 3, 2017. [Online]. Available: https://doi.org/10.3390/mi8030083

[22] T. W. Gilbert, “Strategies for tissue and organ decellularization,” Journal of Cellular Biochemistry, vol. 112, no. 7, 2012. [Online]. Available: https://doi-org.ludwig.lub.lu.se/10.1002/jcb.24130

[23] M. Klak, I. Łojszczyk, A. Berman, G. Tymicki, A. Adamiok-Ostrowska, M. Sierakowski, R. Olkowski, A. A. Szczepankiewicz, A. Kaminksi, A. Dobrzyn, and M. Wszoła, “Impact of porcine pancreas decellularization conditions on the quality of obtained decm,” International Journal of Molecular Sciences, vol. 22, no. 7005, 2021. [Online]. Available: https://doi.org/10.3390/ijms22137005

[24] G. R. Liguori, T. T. A. Liguori, S. R. de Moraes, V. Sinkunas, V. Terlizzi, J. A. van Dongen, P. K. Sharma, L. F. P. Moreira, and M. C. Harmsen, “Molecular and biomechanical clues from cardiac tissue decellularized extracellular matrix drive stromal cell plasticity,” Frontiers in Bioengineering and Biotechnology, vol. 8, no. 520, 2020. [Online]. Available: https://doi.org/10.3389/fbioe.2020.00520

[25] S. R. Meyer, B. Chiu, T. A. Churchill, L. Zhu, J. R. Lakey, and D. B. Ross, “Comparison of aortic valve allograft decellularization techniques in the rat,” Journal of Biomedical Research Part A, vol. 79A, no. 2, pp. 254–262, 2006. [Online]. Available: https://doi-org.ludwig.lub.lu.se/10.1002/jbm.a.30777

[26] D. O. Freytes, J. Martin, S. S. Velankar, A. S. Lee, and S. F. Badylak, “Preparation and rheological characterization of a gel form of the porcine urinary bladder matrix,” Biomaterials, vol. 29, no. 11, pp. 1630–1637, 2008.

[27] Mass spectrometry Facility, 2023. *Project number MS-23-025*. Internal report (Uppsala University). Unpublished.

Appendix

Notes

1. If there is a significant loss of mass after a wash, the tissue may need to be reweighed to adjust volume of the following steps.
2. To separate the tissue from the washing liquid, strain excess solution with a filter and transfer tissue using tweezers.
3. Can preferably be prepared at least one day prior to use, as Triton X-100 takes some time to dissolve in water. Heating the mixture speeds up the process.
4. Ratio of dECM to solution depends on the tissue used and desired properties of the gel. For dECM from porcine skin, a concentration of at least 30 mg/ml is suggested. For heart and aorta, a maximum concentration of 7.5 mg/ml is enough.
5. The standard procedure suggests a time of 48 hours, but this can be extended if necessary.
6. For tissues containing a lot of fat, e.g. skin, gentle revolving is paramount for a functioning gel. If this is not possible, it is preferred to omit revolving and instead intermittently shake the container.
7. The starting pH of the pre-gel should be between 2 and 3. To reach 7.2, about 1-1.5 drops per ml of pre-gel is needed. When approaching a pH of 6, a NaOH solution of lower concentration is preferred to avoid a sudden sharp increase of pH. If that happens, the pH of the pre-gel can be adjusted down with 25 % acetic acid.
8. When the pepsin is inactivated at pH 6.5, the pre-gel will start to gel if it heats up. An ice water bath and repeated mixing is suggested.
9. The container used should be lipophilic, e.g. polypropylene, as the greasy residue will stick to it and help with separation.
10. Note that the properties of the pre-gel can change over time.

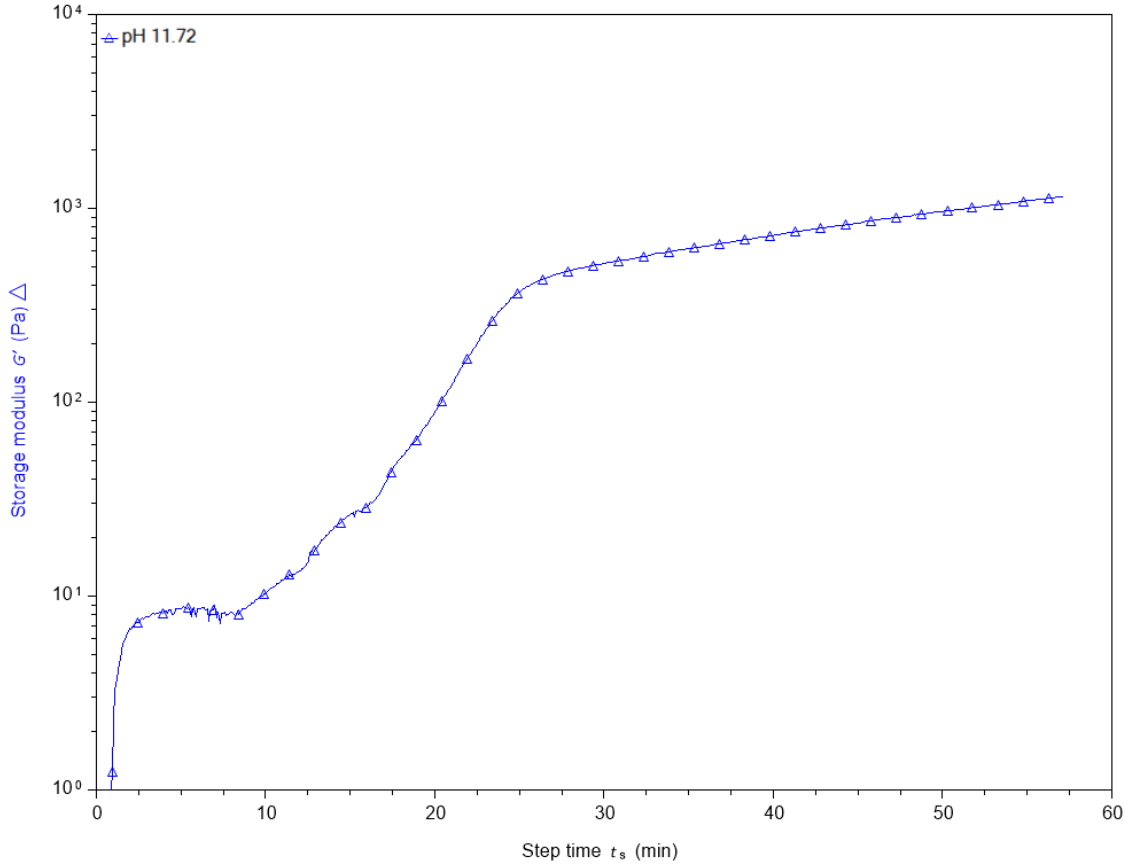

Figure A1: Storage modulus of gel made from sdECM when heated to 37 ℃.

a)

Accession	Description	Score	Coverage	# Proteins	# Unique Peptides	# Peptides	# PSMs	# AAs
A0A4X1USL6	Collagen alpha-1(I) chain OS=Sus scrofa OX=9823 PE=4 SV=1 - [A	106,15	9,45	7	11	11	37	1449
A0A8D0N0P9	Fibrillin-1 OS=Sus scrofa OX=9823 GN=FBN1 PE=3 SV=1 - [A0A8D	105,20	16,38	12	34	37	59	2735
A0A8D1AM50	Fibrillar collagen NC1 domain-containing protein OS=Sus scrofa OX	41,66	4,61	9	4	4	18	1128
A0A8D1RUK6	IF rod domain-containing protein OS=Sus scrofa OX=9823 PE=3 S	36,63	19,13	17	8	12	20	507
A0A8X9AEL6	Collagen type I alpha 2 chain OS=Sus scrofa OX=9823 GN=COL1A2	35,42	10,20	4	11	11	16	1363
A0A8D0KJ64	IF rod domain-containing protein OS=Sus scrofa OX=9823 PE=3 S	28,83	12,37	11	7	8	19	574
A0A8D0XUB4	Keratin, type I cytoskeletal 14 OS=Sus scrofa OX=9823 GN=LOC11	28,15	23,40	7	8	12	16	483
A0A8D0RLB7	Fibrillin-2 OS=Sus scrofa OX=9823 PE=3 SV=1 - [A0A8D0RLB7_PI	27,23	6,36	12	12	16	20	2753
P00761	Trypsin OS=Sus scrofa OX=9823 PE=1 SV=1 - [TRYP_PIG]	26,28	16,45	6	3	3	13	231
A0A4X1WBN6	IF rod domain-containing protein OS=Sus scrofa OX=9823 PE=3 S	16,85	8,15	8	1	6	9	589
A0A8D0Q551	Latent transforming growth factor beta binding protein 4 OS=Sus s	10,80	3,68	14	6	6	6	1521
A0A8D1GGL0	IF rod domain-containing protein OS=Sus scrofa OX=9823 PE=3 S	9,85	14,34	21	6	10	11	544
A0A8D0SNX5	IF rod domain-containing protein OS=Sus scrofa OX=9823 GN=KR	9,40	8,07	10	4	5	5	632
A0A8D0K994	IF rod domain-containing protein OS=Sus scrofa OX=9823 PE=3 S	9,18	7,28	11	2	5	6	536
A0A8W4FKS5	Actin alpha 2, smooth muscle OS=Sus scrofa OX=9823 GN=ACTA2	5,92	21,26	38	6	6	6	334
G8FUN3	Elastin (Fragment) OS=Sus scrofa OX=9823 PE=2 SV=1 - [G8FUN	5,52	21,80	37	2	2	2	133
A0A8D1BCS7	VWFC domain-containing protein OS=Sus scrofa OX=9823 PE=4 S	4,89	1,18	18	2	2	2	849
A0A8D1UFP2	Histone H4 OS=Sus scrofa OX=9823 PE=3 SV=1 - [A0A8D1UFP2_F	4,87	22,09	6	2	2	2	163
A0A480KDW5	Collagen alpha-3(VI) chain isoform 4 OS=Sus scrofa OX=9823 PE=	4,22	1,73	43	3	3	4	2139
A0A4X1TBM2	Peptidase A1 domain-containing protein OS=Sus scrofa OX=9823 F	3,79	5,88	6	2	2	3	391
A0A8D0WM31	Albumin domain-containing protein OS=Sus scrofa OX=9823 PE=4	3,66	10,23	38	6	6	6	528
I3LQ84	Collagen type VI alpha 2 chain OS=Sus scrofa OX=9823 GN=COL6A	2,45	1,81	25	2	2	2	938
P45846	Dermatopontin OS=Sus scrofa OX=9823 GN=DPT PE=1 SV=2 - [DI	2,43	10,38	3	2	2	2	183
A0A8D0K582	Fibulin 5 OS=Sus scrofa OX=9823 GN=FBLN5 PE=4 SV=1 - [A0A8D	2,18	4,27	18	2	2	2	422
A0A4X1T2Z5	chitinase OS=Sus scrofa OX=9823 PE=3 SV=1 - [A0A4X1T2Z5_PIG	2,10	11,67	11	3	3	4	317
A0A8D0LUV4	IF rod domain-containing protein OS=Sus scrofa OX=9823 PE=3 S	1,97	6,15	7	2	4	5	455
A0A8D0JFY6	Ornithine transcarbamylase, mitochondrial OS=Sus scrofa OX=982	1,76	5,49	1	2	2	3	328
A0A4X1VKD2	Calponin OS=Sus scrofa OX=9823 GN=CNN1 PE=3 SV=1 - [A0A4X	1,69	8,10	8	2	2	2	247
A0A286ZJ45	EGF containing fibulin extracellular matrix protein 1 OS=Sus scrofa	1,63	7,86	16	3	3	3	458
A0A8D0U986	Myosin motor domain-containing protein OS=Sus scrofa OX=9823	1,61	2,43	35	2	2	2	781
A0A8D0K8K2	SH3 domain-containing protein OS=Sus scrofa OX=9823 PE=4 SV=	1,61	1,09	18	3	3	3	1927

b)

Accession	Description	Score	Coverage	# Proteins	# Unique Peptides	# Peptides	# PSMs	# AAs
A0A4X1U902	Titin OS=Sus scrofa OX=9823 PE=3 SV=1 - [A0A4X1U902_PIG]	533,02	14,92	8	330	330	379	26898
A0A8D0N3I6	Fibrillin-1 OS=Sus scrofa OX=9823 GN=FBN1 PE=3 SV=1 - [A0A8D	311,07	31,59	8	68	69	185	2776
A0A286ZPX6	Myosin heavy chain 7 OS=Sus scrofa OX=9823 GN=MYH7 PE=3 SV	257,47	33,30	26	64	64	151	1913
A0A4X1USL6	Collagen alpha-1(I) chain OS=Sus scrofa OX=9823 PE=4 SV=1 - [A	92,53	10,35	7	11	11	36	1449
A0A8D1FLQ4	Tropomyosin alpha-1 chain OS=Sus scrofa OX=9823 PE=3 SV=1 -	45,07	38,38	7	8	15	25	284
A0A8D0RLB7	Fibrillin-2 OS=Sus scrofa OX=9823 PE=3 SV=1 - [A0A8D0RLB7_PI	41,85	10,17	12	21	23	33	2753
A0A8D1RUK6	IF rod domain-containing protein OS=Sus scrofa OX=9823 PE=3 SV	38,21	17,36	17	8	10	17	507
A0A8D0XVY6	Heparan sulfate proteoglycan 2 OS=Sus scrofa OX=9823 GN=HSPG	35,46	6,89	22	21	21	22	4051
A0A8D1AM50	Fibrillar collagen NC1 domain-containing protein OS=Sus scrofa OX	34,02	2,66	9	2	2	14	1128
A0A8X9AEL6	Collagen type I alpha 2 chain OS=Sus scrofa OX=9823 GN=COL1A2	33,86	9,24	4	10	10	18	1363
A0A4X1VW25	Tropomyosin 2 OS=Sus scrofa OX=9823 GN=TPM2 PE=3 SV=1 - [	28,42	27,46	5	1	12	14	284
A0A480TDT7	Calcium-transporting ATPase OS=Sus scrofa OX=9823 PE=3 SV=1	25,71	16,91	14	14	14	20	940
A0A8D0S2S8	Myosin-binding protein C, cardiac-type OS=Sus scrofa OX=9823 PE	23,97	14,13	20	16	16	21	1274
P00761	Trypsin OS=Sus scrofa OX=9823 PE=1 SV=1 - [TRYP_PIG]	19,97	30,30	6	5	5	13	231
A0A8D0ZC00	Keratin, type I cytoskeletal 17 OS=Sus scrofa OX=9823 GN=LOC10	19,87	17,69	15	5	7	9	407
A0A480HYV8	Fibronectin OS=Sus scrofa OX=9823 PE=4 SV=1 - [A0A480HYV8_P	19,87	10,52	28	18	18	18	2177
A0A8D0MBC1	ATP synthase subunit alpha OS=Sus scrofa OX=9823 GN=ATP5F1A	19,75	17,25	18	9	9	10	539
A0A480KDW5	Collagen alpha-3(VI) chain isoform 4 OS=Sus scrofa OX=9823 PE=	19,17	5,80	43	10	10	15	2139
A0A4X1V648	Actin, aortic smooth muscle OS=Sus scrofa OX=9823 GN=ACTA2 P	18,54	29,41	27	1	8	14	340
A0A287BF33	Actin, alpha skeletal muscle OS=Sus scrofa OX=9823 GN=ACTA1 P	18,54	29,15	10	1	8	14	343
A0A8W4FN21	ADP/ATP translocase OS=Sus scrofa OX=9823 GN=SLC25A4 PE=1	16,91	22,55	8	7	7	11	275
A0A4X1T5V8	VWFA domain-containing protein OS=Sus scrofa OX=9823 PE=4 S	15,46	6,08	31	5	5	7	823
P67937	Tropomyosin alpha-4 chain OS=Sus scrofa OX=9823 GN=TPM4 PE	13,46	25,00	1	1	8	9	248
A0A8D0KJ64	IF rod domain-containing protein OS=Sus scrofa OX=9823 PE=3 SV	12,59	10,28	11	5	6	10	574
A0A4X1WBN6	IF rod domain-containing protein OS=Sus scrofa OX=9823 PE=3 SV	12,38	7,81	8	1	5	8	589
Q0QF26	Malate dehydrogenase (Fragment) OS=Sus scrofa OX=9823 GN=M	11,86	13,48	13	3	3	5	282
A0A286ZJ45	EGF containing fibulin extracellular matrix protein 1 OS=Sus scrofa	11,51	15,50	16	6	6	7	458
Q0QEM6	ATP synthase subunit beta (Fragment) OS=Sus scrofa OX=9823 GI	11,48	18,08	9	6	6	8	437
A0A8D0NM44	Plasminogen OS=Sus scrofa OX=9823 PE=3 SV=1 - [A0A8D0NM44	11,36	10,27	35	6	6	7	672
A0A4X1UGJ3	carnitine O-palmitoyltransferase OS=Sus scrofa OX=9823 GN=CPT	11,27	5,45	9	4	4	5	734
A0A8D1S785	Voltage-dependent anion-selective channel protein 2 OS=Sus scrof	11,19	25,37	6	5	5	6	272
A0A8D1E3E8	VWFC domain-containing protein OS=Sus scrofa OX=9823 PE=4 S	10,67	3,32	13	4	4	5	1174
A0A4X1TA63	chitinase OS=Sus scrofa OX=9823 GN=CHIA PE=3 SV=1 - [A0A4X	10,58	9,64	10	4	4	7	477
A0A8D0I1Z6	Myomesin 1 OS=Sus scrofa OX=9823 GN=MYOM1 PE=4 SV=1 - [A	10,37	6,99	16	11	11	11	1546
A0A8D0Z4V1	Laminin subunit gamma-1 OS=Sus scrofa OX=9823 PE=4 SV=1 - [	10,21	9,79	30	9	9	9	1358
A0A8D0N517	IF rod domain-containing protein OS=Sus scrofa OX=9823 PE=3 SV	9,93	9,88	25	3	6	6	567
A0A480R601	Cysteine and glycine-rich protein 3 OS=Sus scrofa OX=9823 PE=4	8,85	31,64	4	4	4	5	177
A0A4X1TBM2	Peptidase A1 domain-containing protein OS=Sus scrofa OX=9823 P	8,75	5,88	6	3	3	5	391
A0A8D0SIW3	Laminin subunit beta-2 OS=Sus scrofa OX=9823 PE=4 SV=1 - [A0	8,72	6,64	21	7	7	7	1430
A0A8D0SNX5	IF rod domain-containing protein OS=Sus scrofa OX=9823 GN=KRT	8,49	5,85	10	3	4	4	632
A0A8D1KCR8	VWFA domain-containing protein OS=Sus scrofa OX=9823 PE=4 S	8,38	5,21	10	4	4	8	959
A0A480VP53	Fibulin-5 isoform X3 OS=Sus scrofa OX=9823 PE=4 SV=1 - [A0A48	8,37	6,96	15	3	3	4	431
A0A5G2QN32	Actinin alpha 2 OS=Sus scrofa OX=9823 GN=ACTN2 PE=1 SV=1 -	7,57	12,19	8	11	11	11	894
A0A287BL23	Isocitrate dehydrogenase [NADP] OS=Sus scrofa OX=9823 GN=IDH	7,12	7,84	9	3	3	5	421
A0A287AH53	Four and a half LIM domains 2 OS=Sus scrofa OX=9823 GN=FHL2	6,76	18,64	5	5	5	5	279
A0A4X1SRL8	Elongation factor 1-alpha OS=Sus scrofa OX=9823 GN=EEF1A2 PE	6,51	11,74	31	5	5	6	443
A0A480VFZ6	Laminin subunit beta-1 OS=Sus scrofa OX=9823 PE=4 SV=1 - [A0	6,24	2,55	35	4	4	4	1609
A0A481CCJ1	Glyceraldehyde-3-phosphate dehydrogenase OS=Sus scrofa OX=9	6,03	18,32	6	6	6	9	333
A0A8D1Y994	Voltage-dependent anion-selective channel protein 1 OS=Sus scrof	5,86	12,69	13	2	3	4	268
A0A4X1VZK6	Myomesin 2 OS=Sus scrofa OX=9823 GN=MYOM2 PE=4 SV=1 - [A	5,14	6,38	18	8	8	8	1349
A0A8D1VQA7	Desmin OS=Sus scrofa OX=9823 GN=DES PE=3 SV=1 - [A0A8D1V	4,98	6,94	5	3	3	3	432
A0A8D0J8D6	Collagen IV NC1 domain-containing protein OS=Sus scrofa OX=982	4,97	2,18	28	3	3	4	1649
A0A480MYX8	Laminin subunit alpha-5 isoform X1 OS=Sus scrofa OX=9823 PE=4	4,90	1,46	13	3	3	3	2802
I6XPV3	Voltage-dependent anion channel 3 (Fragment) OS=Sus scrofa OX	4,84	20,61	4	3	4	5	262
A0A8D0LHJ3	LIM zinc-binding domain-containing protein OS=Sus scrofa OX=982	4,72	13,15	26	3	3	3	251
A0A8W4FBE9	Albumin OS=Sus scrofa OX=9823 GN=ALB PE=4 SV=1 - [A0A8W4I	4,61	12,15	35	5	5	5	395
A0A8D1EHZ6	3-hydroxybutyrate dehydrogenase 1 OS=Sus scrofa OX=9823 PE=3	4,52	10,38	7	3	3	3	318
A0A4X1TJ70	Succinate dehydrogenase [ubiquinone] flavoprotein subunit, mitoch	4,51	11,31	12	5	5	5	566
A0A8D0LIC7	Nidogen 1 OS=Sus scrofa OX=9823 PE=4 SV=1 - [A0A8D0LIC7_PI	4,34	4,01	40	4	4	4	1072
A0A287ALC3	Heterogeneous nuclear ribonucleoproteins A2/B1 OS=Sus scrofa O	4,31	9,96	32	3	3	3	261
A0A8D0UTD5	Fibrinogen C-terminal domain-containing protein OS=Sus scrofa O	4,28	11,86	3	5	5	5	489
A0A4X1VZ12	Tubulointerstitial nephritis antigen like 1 OS=Sus scrofa OX=9823	4,25	5,44	8	2	2	2	423
P45846	Dermatopontin OS=Sus scrofa OX=9823 GN=DPT PE=1 SV=2 - [D	4,20	14,75	3	3	3	3	183
A0A287AL55	Alpha-1,4 glucan phosphorylase OS=Sus scrofa OX=9823 GN=PYGI	4,19	7,91	29	6	6	6	809
A7E1T1	L-lactate dehydrogenase (Fragment) OS=Sus scrofa OX=9823 PE=	4,18	14,57	14	3	3	3	199
A0A8D0R9F2	Succinate--CoA ligase [ADP-forming] subunit beta, mitochondrial O	4,06	6,91	10	3	3	3	405
A0A8D1KXA4	Integrin beta OS=Sus scrofa OX=9823 GN=ITGB1 PE=3 SV=1 - [A	4,03	3,24	26	2	2	3	741
A0A480QXR0	Protein-glutamine gamma-glutamyltransferase 2 isoform a OS=Sus	3,95	5,69	13	3	3	3	615
A0A8D1KBQ2	ShKT domain-containing protein OS=Sus scrofa OX=9823 PE=3 SV	3,93	10,65	17	2	2	2	169

c)

Accession	Description	Score	Coverage	# Proteins	# Unique Peptides	# Peptides	# PSMs	# AAs
A0A1S7J210	Alpha1 chain of type I collagen OS=Sus scrofa domesticus OX=982	207,09	25,51	5	25	25	75	1466
A0A480SN35	Titin isoform X6 OS=Sus scrofa OX=9823 PE=3 SV=1 - [A0A480SI	153,49	4,06	1	91	91	95	28113
A0A8X9AEL6	Collagen type I alpha 2 chain OS=Sus scrofa OX=9823 GN=COL1A2	79,96	21,35	4	18	18	42	1363
P00761	Trypsin OS=Sus scrofa OX=9823 PE=1 SV=1 - [TRYP_PIG]	77,21	38,96	6	6	6	36	231
A0A8D1RUK6	IF rod domain-containing protein OS=Sus scrofa OX=9823 PE=3 SV	68,22	17,36	17	10	12	27	507
A0A8D1AM50	Fibrillar collagen NC1 domain-containing protein OS=Sus scrofa OX	61,84	8,24	9	6	6	22	1128
A0A8D1MPX1	Fibrillin 1 OS=Sus scrofa OX=9823 PE=3 SV=1 - [A0A8D1MPX1_PI	54,87	11,00	4	24	24	27	2810
A0A8D1CYZ9	Pepsin A OS=Sus scrofa OX=9823 PE=3 SV=1 - [A0A8D1CYZ9_PIG	47,52	3,23	5	2	2	39	371
A0A8D0KJ64	IF rod domain-containing protein OS=Sus scrofa OX=9823 PE=3 SV	38,38	13,76	11	6	8	27	574
A0A8D0XUB4	Keratin, type I cytoskeletal 14 OS=Sus scrofa OX=9823 GN=LOC11	36,08	21,12	7	8	10	15	483
A0A4X1SJS3	Myosin-4 OS=Sus scrofa OX=9823 GN=MYH4 PE=3 SV=1 - [A0A4X	34,80	8,07	19	8	15	16	1934
A0A8D1CQV1	chitinase OS=Sus scrofa OX=9823 PE=3 SV=1 - [A0A8D1CQV1_PI	27,53	18,83	3	7	7	21	478
A0A4X1WBN6	IF rod domain-containing protein OS=Sus scrofa OX=9823 PE=3 SV	27,17	7,81	8	1	5	12	589
A0A8D0N517	IF rod domain-containing protein OS=Sus scrofa OX=9823 PE=3 SV	25,15	18,87	13	6	11	12	567
A0A8D0SNX5	IF rod domain-containing protein OS=Sus scrofa OX=9823 GN=KRT	24,66	9,97	10	5	7	10	632
A0A8D0JIY9	Peptidase A1 domain-containing protein OS=Sus scrofa OX=9823 P	20,66	8,99	6	4	4	11	434
A0A8D0K994	IF rod domain-containing protein OS=Sus scrofa OX=9823 PE=3 SV	18,78	10,63	11	2	6	8	536
A0A4X1T5G0	Albumin domain-containing protein OS=Sus scrofa OX=9823 PE=4	18,28	12,12	34	7	7	8	586
A0A8D0TS91	Calcium-transporting ATPase OS=Sus scrofa OX=9823 PE=3 SV=1	15,13	11,66	22	8	8	9	935
A0A8D0TM73	Myosin-7 OS=Sus scrofa OX=9823 PE=3 SV=1 - [A0A8D0TM73_PI	14,26	4,76	27	1	8	8	1764
A0A8W4F836	Mucin 5AC, oligomeric mucus/gel-forming OS=Sus scrofa OX=982	10,16	1,50	10	3	3	4	2608
A0A481CCJ1	Glyceraldehyde-3-phosphate dehydrogenase OS=Sus scrofa OX=9	9,85	32,43	5	10	10	12	333
Q58GK8	Fatty acid synthase (Fragment) OS=Sus scrofa OX=9823 GN=FASN	8,26	2,12	15	5	5	5	2316
A0A8D0P062	Actin, alpha cardiac muscle 1 OS=Sus scrofa OX=9823 PE=3 SV=1	8,26	17,42	36	5	5	6	333
A0A8D1JB64	Junction plakoglobin OS=Sus scrofa OX=9823 PE=3 SV=1 - [A0A8I	6,26	5,47	13	4	4	4	677
A0A4X1THD9	Granulins domain-containing protein OS=Sus scrofa OX=9823 GN=	5,16	5,19	28	2	2	3	539
A0A4X1VXD5	Myomesin-2 OS=Sus scrofa OX=9823 PE=4 SV=1 - [A0A4X1VXD5	4,71	2,17	19	2	2	2	920
A0A8D0Z4V1	Laminin subunit gamma-1 OS=Sus scrofa OX=9823 PE=4 SV=1 - [	4,28	2,80	30	3	3	3	1358
A0A8D1N726	VWFA domain-containing protein OS=Sus scrofa OX=9823 PE=4 S	4,26	1,26	56	2	2	2	1826
Q28833	von Willebrand factor (Fragment) OS=Sus scrofa OX=9823 GN=VW	4,16	0,85	26	2	2	2	2482
A0A480R256	Latent-transforming growth factor beta-binding protein 4 isoform c	4,06	3,66	40	2	2	2	601
A0A8W4FQJ0	Mucin 6, oligomeric mucus/gel-forming OS=Sus scrofa OX=9823 G	3,00	1,31	5	2	2	2	1371
A0A8D1K111	LIM zinc-binding domain-containing protein OS=Sus scrofa OX=982	2,65	10,95	31	2	2	2	210
A0A8D1Y1Z2	Galectin OS=Sus scrofa OX=9823 PE=4 SV=1 - [A0A8D1Y1Z2_PIG	2,57	18,87	15	2	2	2	106
Q19PY1	Alpha-1,4 glucan phosphorylase (Fragment) OS=Sus scrofa OX=98	2,14	3,15	23	3	3	3	731
A0A480QSH9	Alpha-actinin-3 isoform 1 OS=Sus scrofa OX=9823 PE=4 SV=1 - [A	1,92	4,91	23	2	2	2	468
A0A8D0K8K2	SH3 domain-containing protein OS=Sus scrofa OX=9823 PE=4 SV=	1,67	1,45	18	4	4	4	1927

Figure A2: Results from mass spectrometer on gel from aorta **(a)**, ventricle **(b)**, and skin **(c)** dECM. The gels were prepared, digested, and analysed by the Mass spectrometry Facility at Uppsala University [27].

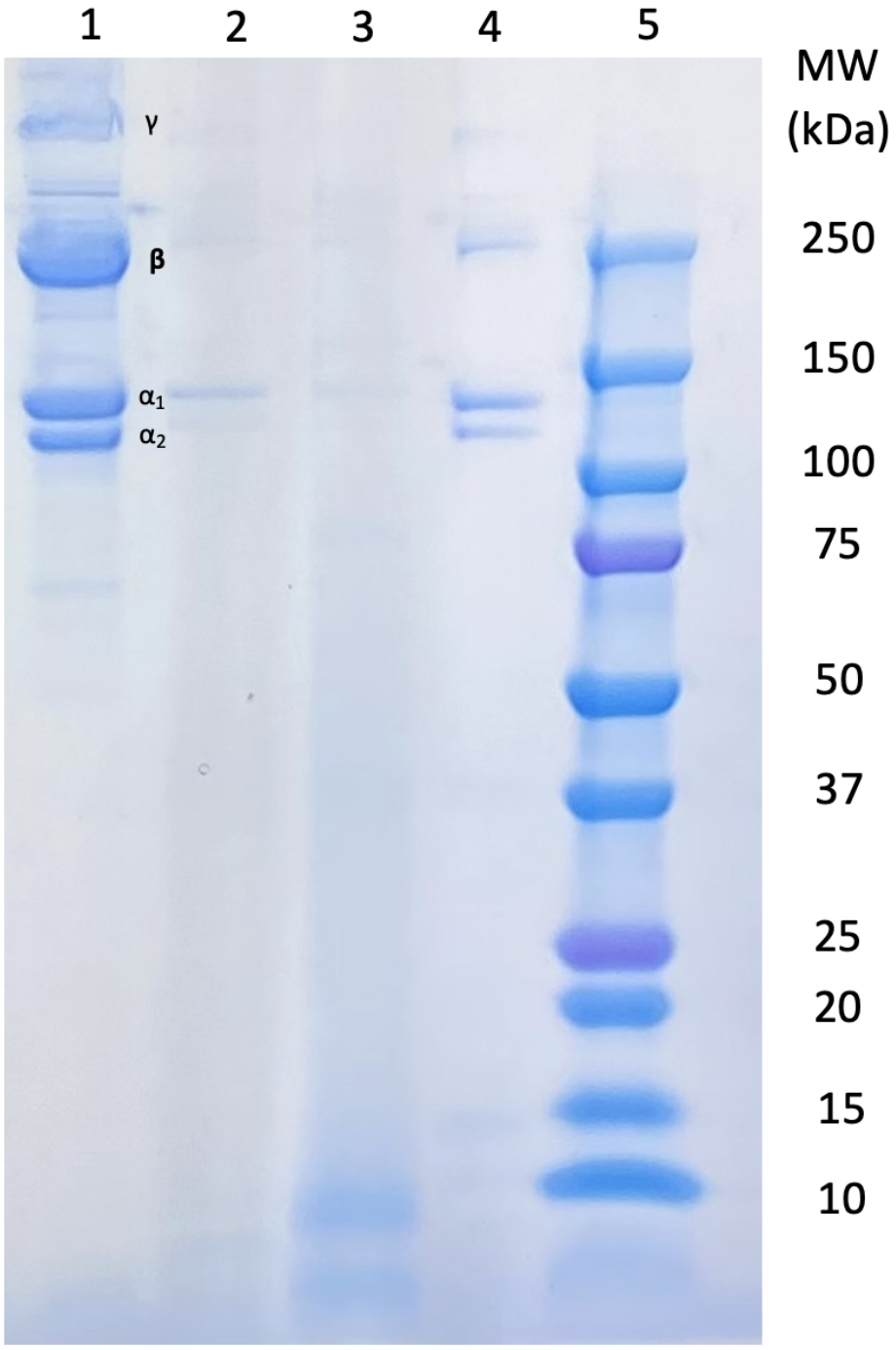

Figure A3: SDS-Page analysis of pregels. Lane 1 is commercial collagen ink, lane 2, 3, and 4 is pregel from aorta, ventricle, and pig skin, respectively. Lane 5 is a protein marker. The gel used is a 4–15% Mini-PROTEAN® TGX™ Precast Protein Gel, the protein marker is Precision Plus Protein Standards Dual Color. Both are from Bio-Rad.